

Systematic study of $(\text{La}_{1-x}\text{Gd}_x)_{1.85}\text{Sr}_{0.15}\text{CuO}_4$ ($0 \leq x \leq 1$): Structure, superconductivity, resistivity, and magnetic properties

Gang Xiao,* Marta Z. Cieplak, and C. L. Chien

Department of Physics and Astronomy, The Johns Hopkins University, Baltimore, Maryland 21218

(Received 28 April 1989)

A room-temperature structural phase diagram has been determined in $(\text{La}_{1-x}\text{Gd}_x)_{1.85}\text{Sr}_{0.15}\text{CuO}_4$ system ($0 \leq x \leq 1$). There exist three stable phases (T , T^* and T'), in which the local Cu-O unit is an octahedron, a pyramid, and a square, respectively. The Jahn-Teller distortion is reduced in the order of T , T^* , and T' . For each phase, there is a solubility region. No magnetic ordering is found in the T and T^* phase, both of which exhibit paramagnetism with a constant Gd magnetic moment consistent with that of Gd^{3+} . In Gd_2CuO_4 and $\text{Gd}_{1.85}\text{Sr}_{0.15}\text{CuO}_4$, the initial susceptibility indicates a Néel state in the Cu-O₂ plane at $T_N=285$ K and another magnetic transition at low temperature. T_N is not sensitive to the Sr doping at all, indicating that extra holes cannot be doped onto the Cu-O₂ plane. While the T^* and T' phases are insulating, exhibiting a variable-range hopping behavior, the Gd-doped $(\text{La}_{1-x}\text{Gd}_x)_{1.85}\text{Sr}_{0.15}\text{CuO}_4$ ($x \leq 0.1$) is superconducting with T_c reducing with increasing Gd concentration. The suppression of T_c is not due to a variation of the electron-boson coupling strength which remains unchanged in the system, but correlates closely with the low-temperature resistivity anomaly. Such an anomaly can be best described by a logarithmic temperature dependence.

I. INTRODUCTION

The advent of high-temperature superconductors has greatly challenged our understanding in condensed matter physics. While intensive experimental investigation has yielded the discovery of half a dozen new oxide superconductors and a wealth of properties of these materials,^{1,2} the basic mechanism responsible for the high- T_c superconductivity defies confirmation.^{1,2} It is commonly believed that the Cu-O₂ plane, which exists in all of the cuprate superconductors, plays a paramount role.¹ However, it remains puzzling that many cuprate oxides with the familiar Cu-O₂ planes are not superconducting at all.³⁻⁶ The study of these oxides is of particular interest because it offers important clues to the function of their superconducting counterparts.

Among all of the cuprate superconductors, $\text{La}_{2-x}\text{Sr}_x\text{CuO}_4$ (the 2:1:4 compound) is a unique system. The carrier concentration can be easily changed by doping the Sr^{2+} ions into the La^{3+} site of the parent compound La_2CuO_4 . As a result, T_c first increases, then saturates, and finally decreases, with increasing carrier concentration.⁷ The structure of this system is the simplest of all with only one Cu-O₂ plane per unit cell, in which the copper atom is octahedrally coordinated by oxygen atoms (the T phase). In addition, there exist a series of compounds $L_2\text{CuO}_4$ (Refs. 8-11) (L : light rare-earth elements from Pr to Gd) that share a similar structure with that of La_2CuO_4 , but the copper atom is square-planar coordinated (the T' phase¹¹). While the hole-doped La_2CuO_4 is a high- T_c superconductor without long-range antiferromagnetic order,⁶ the hole-doped $L_2\text{CuO}_4$ compounds are semiconducting with diverse magnetic orders. Comparative study between these systems should help

one to understand the crucial ingredients of a high- T_c superconductor. Recently, it was discovered^{12,13} that some of the $L_2\text{CuO}_4$ compounds become superconducting with $T_c \sim 10-25$ K if the L site is doped by Ce. Electrical transport measurements indicate that the conduction carriers are electrons.^{12,13} This finding not only opens a new door in the search for high- T_c superconductors, but it also offers important insight into the nature of the electronic state of this type of materials.^{14,15}

One of the effective means to study the cuprate superconductors is cation doping by different elements,¹⁶⁻²² which generally induces changes in structure, oxygen ordering, carrier concentration, magnetic properties, and indeed the superconducting properties. The response of various properties to doping allows us to elucidate the role of a particular constituent of a superconductor.¹⁶⁻²⁰ For example, the Y site in $\text{YBa}_2\text{Cu}_3\text{O}_7$ (the 1:2:3 compound) can be substituted fully by many rare-earth elements with large magnetic moments.¹⁶⁻¹⁸ The superconducting properties are not compromised by such a substitution. It indicates that the Y site is virtually electronically isolated from the Cu-O₂ plane, where the superconduction takes place. Such a picture is also supported by band-theory calculations.²³ In the $\text{La}_{1.85}\text{Sr}_{0.15}\text{CuO}_4$ system, however, doping of rare-earth elements on the La site affects T_c with varying degrees²⁴⁻²⁶ Tarascon *et al.*²⁴ and Takagi *et al.*²⁵ have measured T_c of various samples doped with equal amounts of rare-earth elements. It was found that the light and heavy rare-earth elements reduce T_c slightly, but the intermediate rare-earth elements such as Gd and Tb strongly deteriorate T_c . For example, the T_c of a sample doped with 5 at. % Tb is reduced from 38 to about 26 K. Crabtree *et al.*²⁶ have measured the $(dH_{c2}/dT)_{T_c}$ of two Nd doped sam-

ples, and found no evidence of an exchange interaction between magnetic moments and conduction electrons. Takagi *et al.*²⁵ also concluded that the depression of T_c cannot be ascribed to the magnetic effects, nor to a volume effect as suggested by Tarascon *et al.*²⁴ However, it remains unclear what mechanism is responsible for the T_c suppression.

We have carried out a systematic study of the $(\text{La}_{1-x}\text{Gd}_x)_{1.85}\text{Sr}_{0.15}\text{CuO}_4$ system over the entire composition range of $0 \leq x \leq 1$, in which all three stable phases (T , T^* , T') have been realized. We have determined the structural phase diagram and the superconducting-normal-state phase diagram. The different Cu-O polyhedrons in these phases have profound consequences on carrier doping, conductivity, magnetic characteristics, and indeed superconductivity. The effect of Gd on the superconducting and normal-state properties has been investigated by susceptibility and resistivity measurements. The electron transport and magnetic characteristics of other phases in the system have also been studied.

II. EXPERIMENT

All of the samples used in this study were made by using a standard solid-state reaction method. Appropriate amounts of La_2O_3 , SrCO_2 , Gd_2O_3 , and CuO were well mixed and pressed into pellets. The samples were annealed in an oxygen atmosphere at 1050°C for about 100 h with three intermediate grindings and pressings.

The resulting pellets were cut into regular stripes for four-probe resistivity measurement. Fine copper wires were attached to the samples using silver paint. A computer controlled data-logger system collected the resistivity data as a function of temperature. A SQUID magnetometer was used to measure the temperature dependence of magnetization in both the zero-field-cooled and field-cooled modes, as well as the magnetic susceptibility

in the normal state.

The quality of the samples and the lattice parameters of various phases were determined by using a Phillips APD 3720 automated x-ray powder diffractometer. The scattering angle 2θ ranged from 5° to 80° . The shapes of the diffraction peaks were fitted by a modified Gaussian function. The lattice parameters were then calculated from the positions of at least 22 diffraction peaks using a standard least-squares reduction method.

III. EXPERIMENTAL RESULTS AND DISCUSSIONS

A. Structures and lattice parameters

A series of samples with formula $(\text{La}_{1-x}\text{Gd}_x)_{1.85}\text{Sr}_{0.15}\text{CuO}_4$ ($0 \leq x \leq 1$) and Gd_2CuO_4 were made in order to determine the structural phase diagram of this system. The structures of the two end members without Sr, La_2CuO_4 and Gd_2CuO_4 , are well known. La_2CuO_4 contains two-dimensional planes of Cu-O octahedra (the T phase), and Gd_2CuO_4 consists of planes of Cu-O squares with no apical oxygen atoms (the T' phase).¹¹ Their structures are shown in Figs. 1(a) and 1(c), respectively. Doping Sr into the La or Gd site does not affect the atomic arrangement of the T and T' phases, but reduces the transition temperature from tetragonal to orthorhombic structure in the T phase.²⁷ The T' phase remains tetragonal with Sr doping as will be shown shortly.

A complete solid solution with $0 \leq x \leq 1$ does not exist. Instead we have obtained a structural phase diagram at room temperature as shown in Fig. 2(a). Other than the two stable phases (T and T') at both ends of the phase diagram, there is a new phase with a stoichiometry of $(\text{La}_{0.55}\text{Gd}_{0.45})_{1.85}\text{Sr}_{0.15}\text{CuO}_4$. This phase, whose structure is shown in Fig. 1(b), is the T^* phase consisting of two-dimensional planes of Cu-O pyramids. Such a phase has

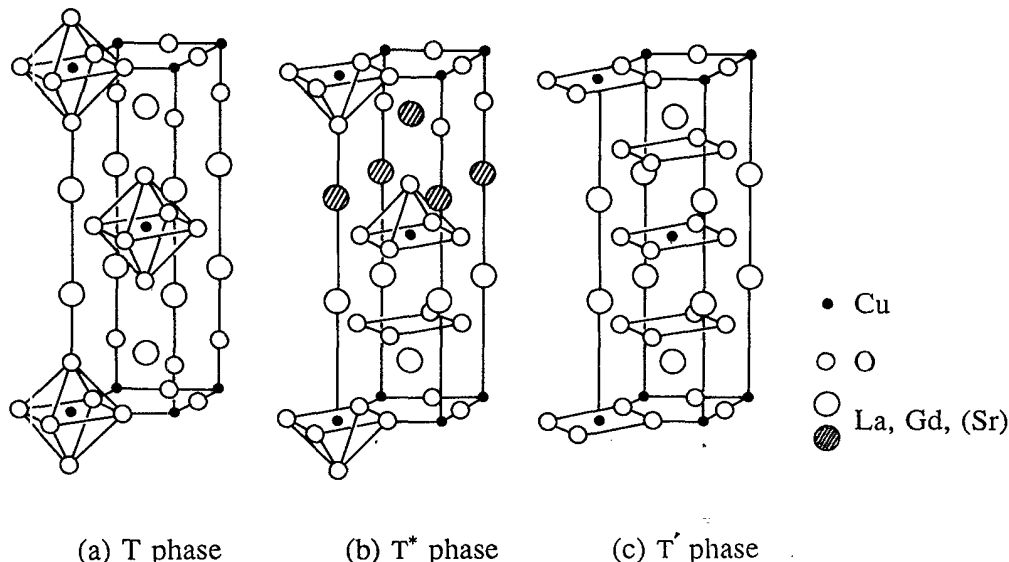


FIG. 1. Structures of (a) the T phase: $\text{La}_{1.85}\text{Sr}_{0.15}\text{CuO}_4$, (b) the T^* phase: $(\text{La}_{0.55}\text{Gd}_{0.45})_{1.85}\text{Sr}_{0.15}\text{CuO}_4$, and (c) the T' phase: $\text{Gd}_{1.85}\text{Sr}_{0.15}\text{CuO}_4$.

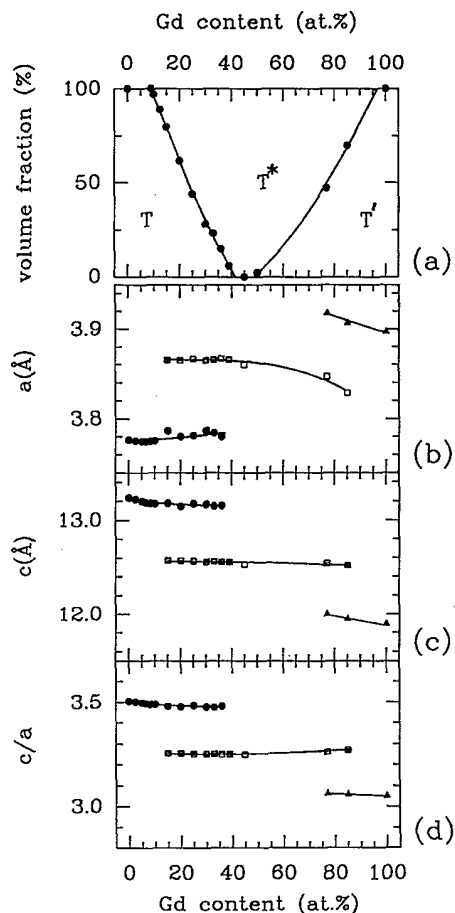


FIG. 2. (a) Structural phase diagram of $(\text{La}_{1-x}\text{Gd}_x)_{1.85}\text{Sr}_{0.15}\text{CuO}_4$. (b)–(d) Lattice parameters a , c , and ratio c/a vs Gd content.

also been observed in $(\text{Nd}_{0.66}\text{Sr}_{0.205}\text{Ce}_{0.135})_2\text{CuO}_4$ by Sawa *et al.*²⁸ using neutron diffraction. The existence of three distinct local Cu-O units in the $(\text{La}_{1-x}\text{Gd}_x)_{1.85}\text{Sr}_{0.15}\text{CuO}_4$ ($x = 0, 0.45, 1$) system is ideally suited for the study of the effect of local Cu-O units on the electronic and magnetic properties of a two-dimensional structure.

The θ - 2θ x-ray diffraction patterns of the three single-phase samples (T , T^* , and T' phases) are shown in Fig. 3. The quality of the samples is excellent without any observable impurity phases. All the peaks can be indexed with a tetragonal perovskite structure. The three pure phases and their composition ranges found in the $(\text{La}_{1-x}\text{Gd}_x)_{1.85}\text{Sr}_{0.15}\text{CuO}_4$ system are the T phase: $0 \leq x \leq 0.1$, the T^* phase: $0.42 \leq x \leq 0.49$, and the T' phase: $0.95 \leq x \leq 1$. In the composition range bordered by the T and T^* phases or the T^* and T' phases, mixed phases appear with one phase growing at the expense of the other. The volume fraction of various phases in the mixed-phase regions was determined from the relative intensities of the (200) diffraction peaks. The lattice parameters (a and c) of various phases are presented in Figs. 2(b) and 2(c). Lattice parameter a increases and parameter c decreases in the order of T , T^* , and T' . Such a behavior is caused by the diminishing Jahn-Teller distortion,

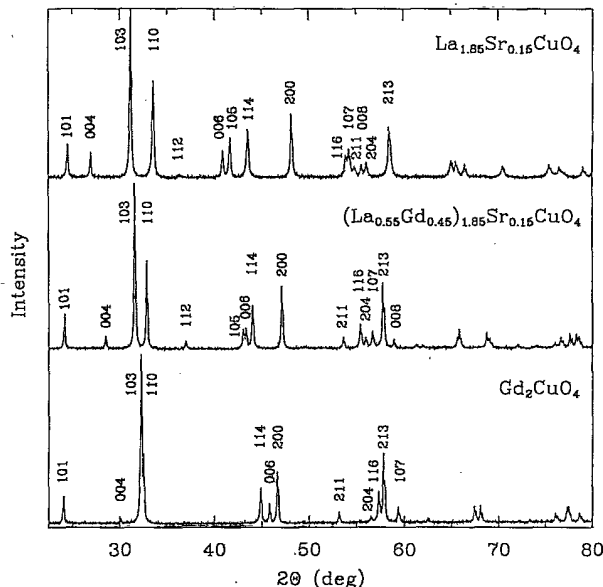


FIG. 3. θ - 2θ x-ray powder diffraction patterns of the T phase $\text{La}_{1.85}\text{Sr}_{0.15}\text{CuO}_4$, the T^* phase $(\text{La}_{0.55}\text{Gd}_{0.45})_{1.85}\text{Sr}_{0.15}\text{CuO}_4$, and the T' phase Gd_2CuO_4 . Every diffraction peak in the three patterns can be indexed with a tetragonal perovskite structure shown in Fig. 1. Here only the main peaks are labeled with indices.

which is the strongest in a Cu-O octahedron. Consequently, there is a consistent reduction in the c/a ratio [Fig. 3(d)] from T to T' phase. Due to the Jahn-Teller distortion, lattice parameter c is generally larger than three times parameter a . But in the order of T , T^* , T' , the c/a ratio decreases from 3.50, to 3.25, and finally to

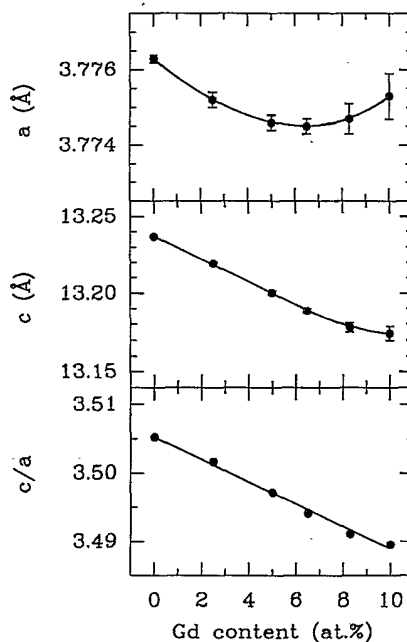


FIG. 4. The variation of the lattice parameters a , c , and the ratio c/a with Gd content in the T phase $(\text{La}_{1-x}\text{Gd}_x)_{1.85}\text{Sr}_{0.15}\text{CuO}_4$ ($0 \leq x \leq 0.1$).

3.05, indicating the gradual reduction of the Jahn-Teller distortion.

The T^* and T' phases with Sr doping are not metallic. In order to study the effect of Gd doping on the superconducting $\text{La}_{1.85}\text{Sr}_{0.15}\text{CuO}_4$ it is meaningful only to investigate those samples in the region of $0 \leq x \leq 0.1$, where the T phase solid solution $(\text{La}_{1-x}\text{Gd}_x)_{1.85}\text{Sr}_{0.15}\text{CuO}_4$ can be formed. Figure 4 shows in detail the lattice parameters in this solid solution region. Gd doping changes lattice parameter a only slightly (less than 0.05%), but shrinks parameter c to a much larger degree (about 0.5%). The c/a ratio decreases linearly with the Gd content.

B. Magnetic susceptibility

We have measured the magnetic susceptibility of all the single-phase samples in the system to determine their magnetic states. It was found that samples of both the T and T^* phases are paramagnetic. The magnetic susceptibility can be well described by the Curie-Weiss law

$$\chi = \chi_0 + \frac{Np_{\text{eff}}^2\mu_B^2}{3k_B(T - \Theta)}, \quad (1)$$

where χ_0 is the temperature-independent part of the susceptibility, N is the number of magnetic ions, p_{eff} is the effective moment in units of Bohr magneton μ_B , and Θ is the Curie-Weiss temperature. Figure 5 shows the inverse of susceptibility as a function of temperature for various Gd-doped T and T^* phase samples. The lines are fits to the data using relation (1). The fitted parameter Θ is

about 0 ± 1 K for the T phase $(\text{La}_{1-x}\text{Gd}_x)_{1.85}\text{Sr}_{0.15}\text{CuO}_4$ with $0 \leq x \leq 0.1$, indicating that the magnetic interaction among the Gd ions is negligibly small. However, in the T^* phase $(\text{La}_{0.55}\text{Gd}_{0.45})_{1.85}\text{Sr}_{0.15}\text{CuO}_4$, the Θ obtained is -9.1 K, a signature of the existence of antiferromagnetic interaction among the Gd ions. The magnetic moment p_{eff} obtained for the Gd^{3+} ions is shown in the inset of Fig. 5 for these samples. The values p_{eff} for both the T and T^* phases remain constant with a value of 7.95, which is identical to $g\sqrt{J(J+1)} = 7.94$, the Gd^{3+} ground-state moment according to Hund's rules.

On the other hand, the T' phase Gd_2CuO_4 and $\text{Gd}_{1.85}\text{Sr}_{0.15}\text{CuO}_4$ exhibit very interesting magnetic orderings, as shown by the susceptibility data in Fig. 6. As a comparison, the data of $(\text{La}_{0.55}\text{Gd}_{0.45})_{1.85}\text{Sr}_{0.15}\text{CuO}_4$ are also included. As shown in Fig. 6 and the inset, two magnetic transitions exist at approximately $T = 285$ and 20 K in the T' phase. The transition at $T_N = 285$ K is undoubtedly associated with the antiferromagnetic ordering of the Cu-O sublattice, similar to the one observed in the La_2CuO_4 with a Néel temperature $T_N \sim 220$ –290 K.^{29–31} The nature of the low-temperature magnetic transition is less clear. Single crystals of Gd_2CuO_4 have recently been studied by Thompson *et al.*⁶ Specific-heat measurement shows a lambda-like anomaly at $T = 6.5$ K, which they regarded as arising from the antiferromagnetic order of the Gd sublattice. The temperature at which a large peak appears in the susceptibility is strongly field dependent, starting at $T_{\text{peak}} = 20$ K in zero field and saturating at $T_{\text{peak}} = 6.5$ K for fields above 5 kG. Because of this, the authors suggested that the low-field T_{peak} at 20 K is not

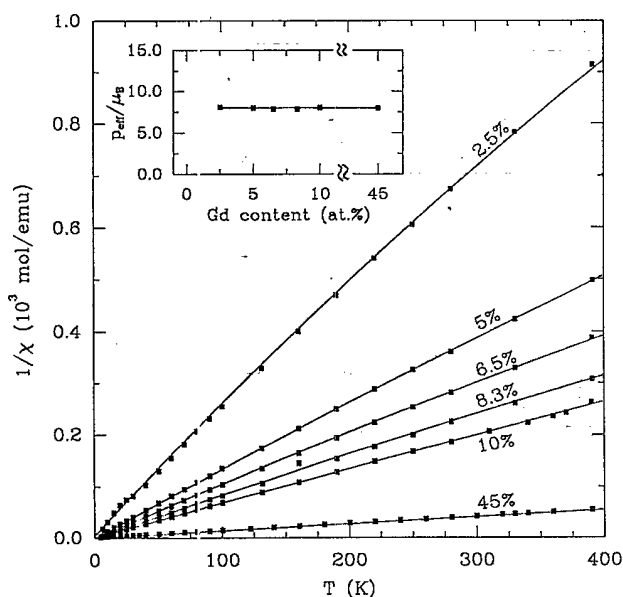


FIG. 5. Temperature dependence of the inverse magnetic susceptibility for samples with the T and T^* phases. The measuring magnetic field is 10 kG. The solid lines are fits to the data using the Curie-Weiss law. The inset shows the magnetic moment of the Gd ion. The value is identical to a moment expected from Gd^{3+} , and it remains constant in the T and T^* phases.

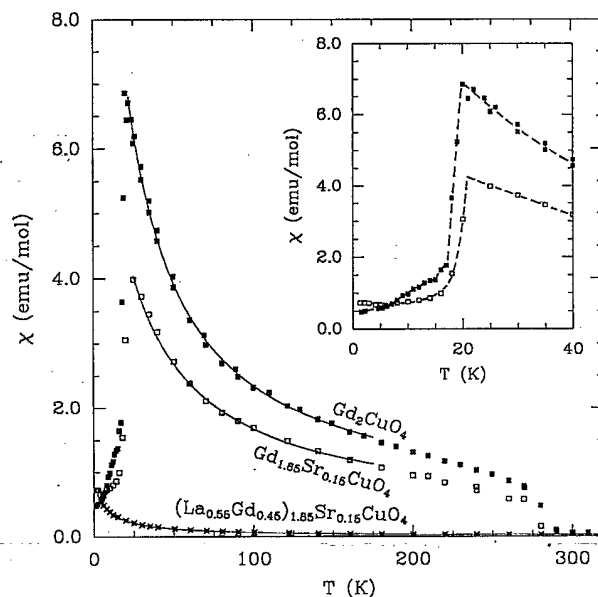


FIG. 6. Temperature dependence of magnetic susceptibility for the T' phase Gd_2CuO_2 and $\text{Gd}_{1.85}\text{Sr}_{0.15}\text{CuO}_4$. The measuring magnetic field is 30 G. The solid lines are fits to the data using the Curie-Weiss law. As a comparison the data for the T^* phase $(\text{La}_{0.55}\text{Gd}_{0.45})_{1.85}\text{Sr}_{0.15}\text{CuO}_4$ are also included. Note that the Néel temperature $T_N = 285$ K is not changed with Sr doping. Inset: susceptibility data at low temperatures.

associated with the antiferromagnetic order of Gd, but is related to the Gd-Cu, Cu-Cu, or other interactions.

In La_2CuO_4 , the Néel state of the Cu sublattice is very susceptible to Ba or Sr doping into the La sites.³¹ T_N is suppressed from 240 K to zero with less than 1 at. % of Sr. However, as shown in Fig. 6, the Néel state of the Cu sublattice in Gd_2CuO_4 is not sensitive to Sr doping at all. T_N remains unchanged with Sr content up to 0.15 (or 7.5 at. %). It is expected that hole doping will significantly affect the magnetism of the Cu sublattice. Holes doped onto the Cu-O₂ planes introduce magnetic frustration,³² and a reduction in Cu-Cu superexchange interaction.³³ All of these effects can destroy the long-range antiferromagnetic ordering effectively. Therefore, the insensitivity of T_N in Gd_2CuO_4 to Sr doping indicates clearly that extra holes are not doped onto the Cu-O₂ plane. As will be shown later, Sr doping in Gd_2CuO_4 does not bring the compound into a metallic state. Hence, the holes introduced by Sr are not mobile and are likely trapped in the vicinity of the local Sr sites. In Gd_2CuO_4 (the T' phase), there are no apical oxygen atoms above and below the Cu sites. The above result suggests that the apical oxygen is required in order for holes to be doped onto the Cu-O₂ planes.

Another interesting observation in Fig. 6 is that the low-field susceptibility ($H = 30$ G) of the T' -phase samples follows a Curie-Weiss behavior in a wide temperature range of $20 < T < 200$ K. The solid lines are fits to the data using relation (1). However, rather surprisingly, the susceptibility is anomalously enhanced over that of the $(\text{La}_{0.55}\text{Gd}_{0.45})_{1.85}\text{Sr}_{0.15}\text{CuO}_4$. The fitted values of p_{eff} and Θ are $31.1(\mu_B)$, -13.1 K and $28.2(\mu_B)$, -20 K for Gd_2CuO_4 and $\text{Gd}_{1.85}\text{Sr}_{0.15}\text{CuO}_4$, respectively. These p_{eff} values are unphysically large for Gd^{3+} ions. Thompson *et al.*⁶ have measured magnetization versus field for Gd_2CuO_4 at temperatures below 270 K. They found a weak-ferromagnetic behavior in the Cu-O₂ planes which induces an internal field of 740 G. This internal field starts to collapse at $T < 18$ K, causing susceptibility to drop abruptly at $T \sim 20$ K (Fig. 6). It was speculated⁶ that such a behavior is a consequence of a lowering of the tetragonal crystal symmetry found at room temperature. Our enhanced low-field susceptibility data is consistent with the existence of an internal field. Assuming a theoretical value of $p_{\text{eff}} = 7.94\mu_B$ for the Gd ions, we have estimated the internal fields to be 460 and 378 G for Gd_2CuO_4 and $\text{Gd}_{1.85}\text{Sr}_{0.15}\text{CuO}_4$, respectively. These internal field values are somewhat lower than that obtained by Thompson *et al.*⁶ This is because the measuring magnetic field (30 G) is not large enough to align the weak-ferromagnetic component of the Cu-O₂ planes.

C. Superconductivity in $(\text{La}_{1-x}\text{Gd}_x)_{1.85}\text{Sr}_{0.15}\text{CuO}_4$ ($x \leq 0.1$)

As mentioned earlier, single-phase solid solutions can be formed within the Gd concentration range of $0 \leq x \leq 0.1$, in which samples are metallic and superconducting. The temperature dependence of the resistivity is shown in Fig. 7 for various samples. At $T > 100$ K, resis-

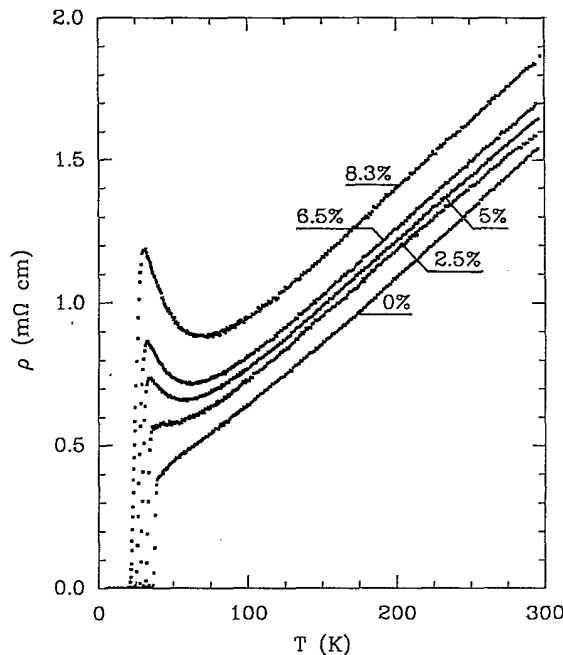


FIG. 7. Temperature dependence of resistivity for samples with various Gd concentrations in the T phase $(\text{La}_{1-x}\text{Gd}_x)_{1.85}\text{Sr}_{0.15}\text{CuO}_4$ ($0 \leq x \leq 0.1$).

tivity increases with Gd concentration, but it follows a linear temperature dependence with essentially identical positive slopes. At lower temperatures (< 75 K), however, a resistivity minimum starts to develop and the resistivity minimum temperature T_{min} rises with increasing Gd concentration (x). Below T_{min} , there is a resistivity

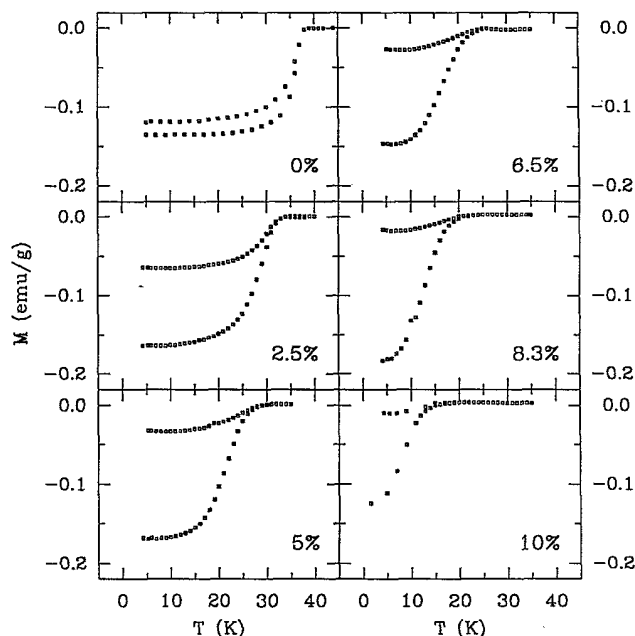


FIG. 8. The variation of magnetization with temperature in the field-cooled and zero-field-cooled mode ($H = 30$ G) for samples with different Gd concentration in the T phase.

upturn whose magnitude also increases with x . These low-temperature resistivity anomalies will be discussed in detail later. As more Gd is doped, T_c decreases steadily from $T_c = 38$ K for the $\text{La}_{1.85}\text{Sr}_{0.15}\text{CuO}_4$ to $T_c = 19$ K for $(\text{La}_{0.9}\text{Gd}_{0.1})_{1.85}\text{Sr}_{0.15}\text{CuO}_4$.

The magnetization of the superconducting samples has been measured in both the zero-field-cooled mode (diamagnetic signal) and the $H = 30$ G field-cooled mode (Meissner signal). As shown in Fig. 8, the diamagnetic signal of the Gd-doped samples remains at a value similar to that of the parent compound, as expected for high-quality samples. However, the Meissner signal reduces gradually with Gd doping. This effect, in our view, is not caused by the structural or electronic inhomogeneity of the samples, but is due to the increasing flux-pinning effect.

The values of T_c determined from magnetization are consistent with those from resistivity data. Figure 9 shows the value of T_c obtained from magnetization measurements for Gd content up to $x = 0.34$. Clearly, the superconducting-normal-state phase diagram is consistent with the structural phase diagram shown in Fig. 2(a). In the single-phase region ($x \leq 0.1$), the value of T_c drops linearly with x . A critical Gd concentration $x_c = 0.2$, above which T_c disappears, can be obtained by extrapolation from the data in the single-phase region. However, above $x = 0.1$, T_c decreases with a different slope from the initial one as samples enter the mixed-phased region.

The T_c suppression behavior in the present 2:1:4 system is in sharp contrast to the ineffectiveness of rare earth R on T_c in the $\text{RBa}_2\text{Cu}_3\text{O}_7$ systems.¹⁶⁻¹⁸ Electroni-

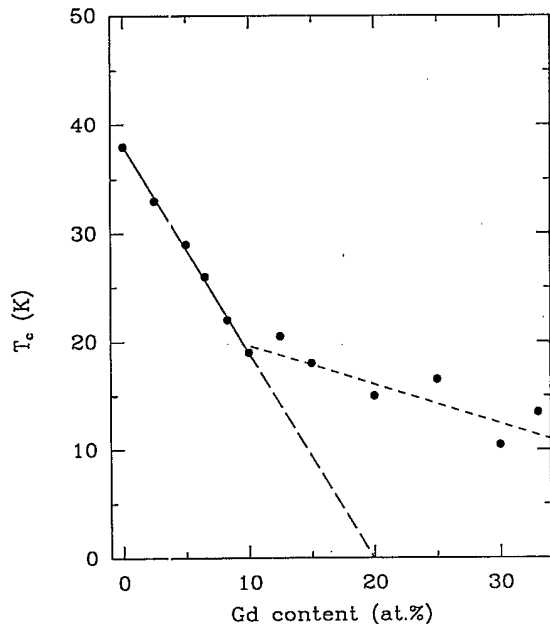


FIG. 9. Gd concentration dependence of the superconducting transition temperature T_c . In the T -phase region ($0 \leq x \leq 0.1$), T_c decreases linearly with Gd content. The critical concentration obtained from extrapolation is $x_c = 0.2$. The change in the slope of T_c above $x = 0.1$ is caused by the appearance of mixed phases.

cally, as in the 1:2:3 compounds, the La site should be well isolated from the Cu-O₂ plane as indicated from band-theory calculations²³ and Mössbauer measurements.²⁶ The exchange interaction between the magnetic moment of Gd and the conduction carriers in the Cu-O₂ planes is too weak to be responsible for the magnetic pair-breaking mechanism. Convincing evidence was provided by Tagaki *et al.*,²⁵ who showed that the nonmagnetic Eu^{3+} affects T_c just as strongly as the Gd^{3+} in the 2:1:4 system. Furthermore, the observed T_c suppression cannot be attributed simply to the reduction in lattice parameters, because, as pointed out by Tagaki *et al.*,²⁵ high-pressure study indicates that T_c in fact increases with decreasing lattice parameters. In the $\text{RBa}_2\text{Cu}_3\text{O}_7$ systems T_c remains at 90 K for a wide range of lattice parameters³⁴ (more than 1% variation). We will further address the mechanism for the T_c suppression in the rare-earth doped 2:1:4 system in the next section.

D. Resistivity and its low-temperature anomaly

The normal-state electronic transport³⁵⁻³⁷ of a superconductor provides valuable information about the nature of electron conduction, coupling strength, elastic and inelastic scattering processes, etc. The superconducting state often correlates intimately with the normal-state properties. In this section, we will examine the resistivity and its low-temperature anomaly in order to elucidate the mechanism for the T_c suppression in the T phase. The temperature dependence of resistivity in the T^* and T' phases will also be discussed.

As can be seen in Fig. 7, the resistivity of the superconducting samples shows a linear temperature dependence at $T > 100$ K, and can be well described by the following relation:

$$\rho = \rho_0 + \rho(x) + \alpha T, \quad T > 100 \text{ K}, \quad (2)$$

where ρ_0 is the residual resistivity due to defects in the parent 2:1:4 compound. $\rho(x)$ is the residual resistivity due to impurity scattering induced by Gd, and the αT term is the temperature-dependent part of the resistivity with α as its slope. The resistivity data in Fig. 7 have been fitted using relation (2), and the obtained parameters $\alpha = d\rho/dT$, $\rho(0 \text{ K}) = \rho_0 + \rho(x)$, and $\rho(297 \text{ K})$ are presented in Fig. 10 as functions of Gd concentration. The straight lines in the figure are least-squares fits to these parameters.

Both Figs. 7 and 10(c) reveal that the slope of the resistivity remains constant as T_c is suppressed by Gd doping. In relation (2), the αT term is caused by the electron-boson (e.g., phonon) scattering, $\alpha T = 4\pi\omega_p^{-2}\tau_{\text{in}}^{-1}$, where ω_p is the plasmon frequency. The inelastic scattering rate τ_{in} is related to the electron-boson coupling strength λ via $\hbar\tau_{\text{in}}^{-1} = 2\pi\lambda k_B T$. Using $\omega_p = (4\pi n e^2 / m^*)^{1/2}$, we obtain

$$\alpha = \frac{d\rho}{dT} = \frac{2\pi k_B}{e^2 \hbar} \frac{m^* \lambda}{n},$$

where n is the carrier concentration and m^* is the effective carrier mass. Therefore, a constant slope suggests that the quantity $(m^* \lambda)/n$ remains constant. Since

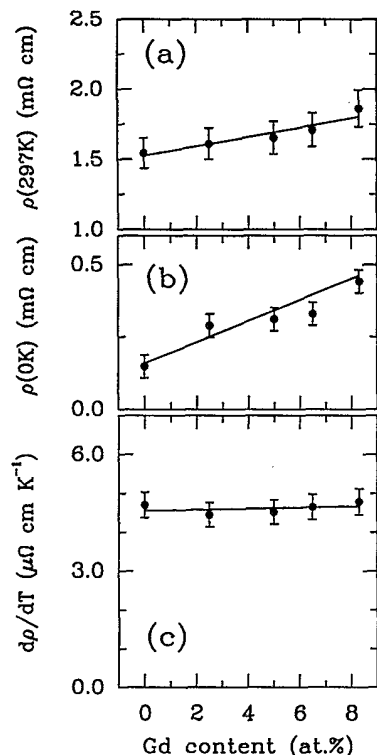


FIG. 10. The variation of (a) the room-temperature resistivity $\rho(297\text{ K})$, (b) the residual resistivity $\rho(0\text{ K})$, and (c) the slope of resistivity $d\rho/dT$ with Gd concentration in the superconducting T phase.

the Gd ion is trivalent, the same as La^{3+} and doping is not in the Cu-O_2 plane, it is not unreasonable to assume that the quantity m^*/n remains unchanged in the low-Gd-doping level ($x \leq 0.1$). Under this assumption, a constant slope of resistivity would imply that the coupling strength (λ) is unaffected by Gd doping. Therefore, the T_c suppression in Fig. 9 is unlikely to be caused by a change in the coupling strength. Furthermore, the inelastic scattering, responsible for the linear temperature dependence, is not the source for the pair breaking.

While the slope of the resistivity remains unchanged, the residual resistivity due to impurity scattering does increase with Gd concentration as shown in Fig. 10(b). At $x = 0.08$, the residual resistivity rises three times over that of the parent 2:1:4 compound. Even though the impurity doping is not in the Cu-O_2 plane, our result clearly shows that local disorder in the Cu-O_2 plane has been induced. As we have shown earlier, the position of the apical oxygen in the local Cu-O octahedron is not stable against Gd doping. In the T^* and T' phases, the number of apical oxygen reduces to 1 and 0, respectively. Therefore, as Gd is doped into the T phase, local structural strain starts to develop until the solubility limit ($x = 0.1$), where the strain is too large for the lattice to be stable. Another evidence of disorder in the Cu-O_2 plane is the decrease of the ratio of the lattice parameters c/a with Gd doping [Fig. 4(c)], which indicates that the Jahn-Teller distortion is weakened.

In conventional superconductors, nonmagnetic disorder has no effect on the T_c of an isotropic superconductor, but is slightly pair breaking in an anisotropic superconductor. Coffey and Cox³⁸ have attempted to calculate the suppression of T_c due to disorder in the high- T_c superconductors. They found that disorder is detrimental to T_c in their model, and T_c will be reduced to about half of its original value T_{c0} , when the mean free path (l), due to disorder decreases to half of the coherence length. It is generally true, regardless of models, that if nonmagnetic disorder is pair breaking, T_c will be affected only when the mean free path is reduced to below the coherence length. Here we will estimate to what extent the disorder is pair breaking in the present system. From the residual resistivity, we can calculate the mean free path according to

$$\rho(0\text{ K}) = \frac{4\pi v_F}{\omega_p^2 l}, \quad (3)$$

where v_F is the Fermi velocity. In $\text{La}_{1.85}\text{Sr}_{0.15}\text{CuO}_4$,³⁵ $\omega_p \approx 0.7\text{ eV}$, $v_F \approx 1 \times 10^7\text{ cm s}^{-1}$, and the coherence length ξ is about 15 \AA . As shown in Fig. 10, $\rho(0\text{ K})$ for the sample with $x = 0.08$ increases to about $450\text{ }\mu\Omega\text{ cm}$, which corresponds to a mean free path of $l = 22\text{ \AA}$. Since $l > \xi$, T_c should not be strongly affected. However, the sample with $x = 0.08$ has a T_c of 22 K , significantly reduced from $T_{c0} = 38\text{ K}$ of the parent compound. Therefore, while disorder may affect T_c to some degree, it is unlikely that the suppression of T_c in the Gd-doped 2:1:4 system is caused by disorder alone. Other mechanisms have to be considered.

Returning to the temperature dependence of resistivity in Fig. 7, we find that the linear temperature dependence seen at $T > 100\text{ K}$ is no longer followed at lower temperatures between T_c and 100 K upon Gd doping. A resistivity minimum and upturn start to appear. Such a resistivity anomaly may result from several sources, for example, temperature-dependent spin-flip scattering, electron

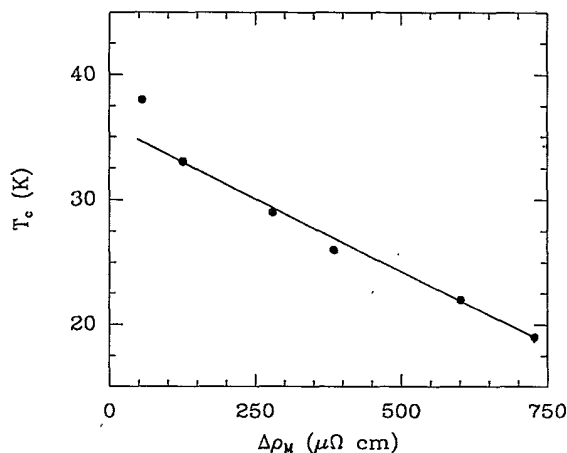


FIG. 11. Correlation between T_c and the magnitude of resistivity upturn $\Delta\rho_M$ at the T_c onset in the T -phase samples ($0 \leq x \leq 0.1$).

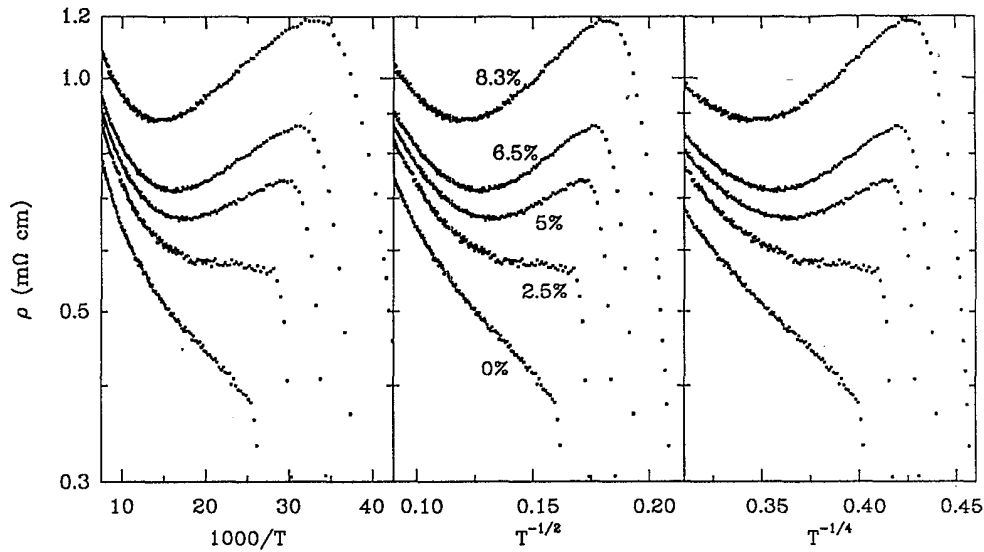


FIG. 12. Resistivity in logarithmic scale vs (a) $1000/T$, (b) $T^{-1/2}$, and (c) $T^{-1/4}$.

localization, activation behavior, variable-range hopping, etc. It is quite possible that the mechanism for the resistivity anomaly is also the one responsible for the suppression of T_c . This is suggested by the following evidence. The magnitude of the resistivity upturn $\Delta\rho(T)$ can be characterized by the

$$\Delta\rho(T) = \rho(T) - \rho_l(T),$$

where $\rho_l(T)$ is the linear temperature dependent part of the resistivity, extrapolated from high temperatures. At the T_c onset, one obtains a maximum upturn $\Delta\rho_M$ for each sample. Interestingly, as we have plotted in Fig. 11, T_c is well correlated with $\Delta\rho_M$ in a linear fashion. This behavior strongly suggests that the suppression of T_c is closely related to the mechanism for the resistivity anomaly.

The cause for the low-temperature resistivity anomaly can be, in principle, inferred from the temperature dependence of resistivity. We first investigate the possibility of a semiconducting behavior or a variable-range hopping process. The resistivity associated with these mechanisms would show a temperature dependence as $\rho \sim \exp(T^{-\beta})$, with $\beta = 1, \frac{1}{4}, \frac{1}{2}$ corresponding, respectively, to activation, uncorrelated and correlated variable-range hopping processes. In Fig. 12, we plot $\ln\rho$ against $T^{-\beta}$. Inspection of the curves reveals that the resistivity upturn in a narrow temperature range can always be marginally fitted by a straight line with a value of β . But there is no temperature range large enough to allow a unambiguous determination of the value of β .

We have attempted to fit the resistivity data with many forms of temperature dependence. To our surprise, the following logarithmic temperature dependence provides excellent fits to our data:

$$\rho(T) = A + BT - C \ln(T), \quad (4)$$

As shown in Fig. 13, where the quantity $(\rho - A - BT)$ is plotted against a $\ln(T)$ scale, the above relation is fol-

lowed in a wide temperature range ($T_c < T < 100$ K). The fitted parameters A , B , and C are presented in Fig. 14 as functions of Gd concentration. Also presented is the ratio C/B which gives the resistivity minimum temperature T_{\min} . All of these parameters increase steadily with Gd doping. The values of T_{\min} obtained from fitting are in good agreement with the experimental values. Overall the low-temperature resistivity anomaly can be described by relation (4) much better than any other tem-

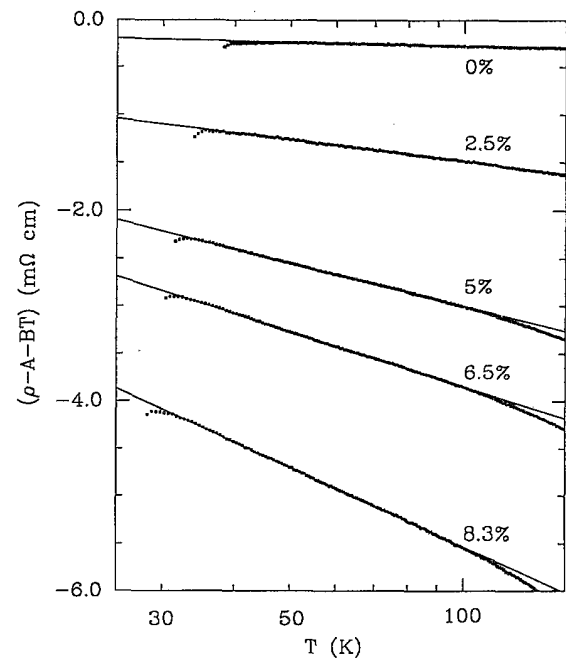


FIG. 13. The dependence of the nonlinear part of the resistivity $\rho - A - BT$ on $\ln(T)$ for samples with various Gd concentrations in the T phase. The solid lines represent the best fits to the data using Eq. (4).

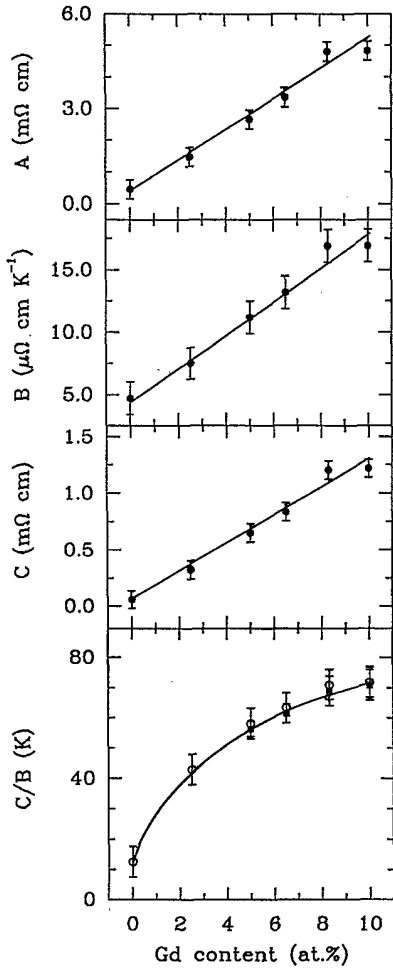


FIG. 14. Variation of the fitted parameters A , B , C , and the ratio C/B with the Gd content. The ratio C/B is the resistivity minimum temperature T_{\min} . The open circles are experimental values of T_{\min} . Note that the fitted values and the experimental values coincide with each other very well.

perature dependence that we are aware of. The key question is the mechanism responsible for the anomaly.

Relation (4) reminds us of two possible mechanisms, the Kondo effect^{39,40} and localization.⁴¹ Both are difficult to rule out. In the $\text{La}_{1.85}\text{Sr}_{0.15}\text{CuO}_4$, localized paramagnetic moment on the Cu site can be readily induced by the introduction of disorder.⁴²⁻⁴⁴ For example, doping on the Cu site by Ga or Zn impurities^{42,43} induces a paramagnetic moment on the neighboring Cu sites. Neutron irradiation which introduces disorder in a lattice also produces a Curie-Weiss behavior in the cuprate superconductors. In the present system, Gd doping on the La site generates appreciable amounts of disorder in the Cu-O₂ plane, as revealed in the residual resistivity. It is possible that such a disorder could cause localization of electrons or induce localized moments on the Cu sites that scatter conduction carriers. Both localization and paramagnetic moment⁴⁵ are possible sources for the T_c suppression. A confirmation or negation of either mechanism needs further experimental evidence other than the present resistivity data. Measurements of magnetoresis-

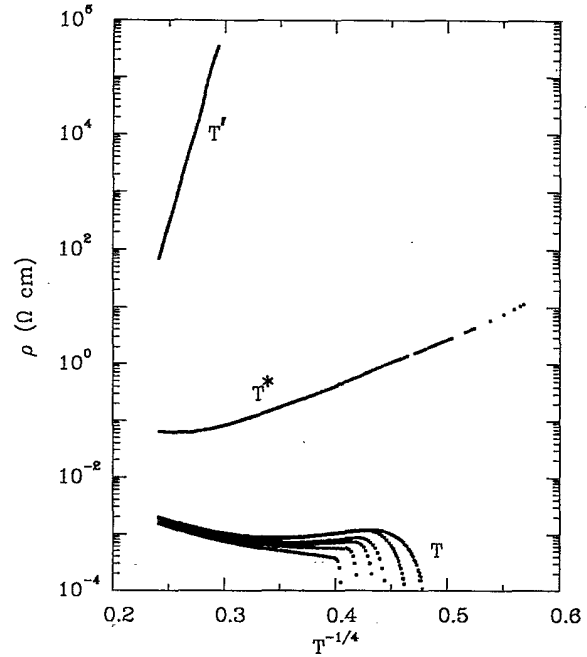


FIG. 15. Resistivity in logarithmic scale vs $T^{-1/4}$ for the T phase ($0 \leq x \leq 0.1$), the T^* phase ($x = 0.45$), and the T' phase ($x = 1$) samples, $(\text{La}_{1-x}\text{Gd}_x)_{1.85}\text{Sr}_{0.15}\text{CuO}_4$.

tance and other transport properties are planned.

As we increase the Gd concentration to near 50 and 100%, two new stable phases T^* and T' are obtained as shown earlier. Even when these two phases are heavily doped with Sr up to at least 0.15 per unit cell, they remain insulating nevertheless. In Fig. 15, we show the resistivity data of the T , T^* , and T' phases against a $T^{-1/4}$ temperature scale, where all the samples have a Sr content of 0.15. Clearly, the conduction mechanism of the T^* and T' is the variable-range hopping. The resistivities of these three phases differ by many orders of magnitude. With increasing Gd concentration, conduction carriers become increasingly more difficult to be doped onto the Cu-O₂ plane. This is consistent with the observation earlier that the Néel temperature T_N in the T' phase $\text{Gd}_{2-x}\text{Sr}_x\text{CuO}_4$ does not depend on the Sr content at all, hence the doped holes are absent in the Cu-O₂ plane. This behavior is most likely caused by the displacement of the apical oxygen atoms in both the T^* and T' phases. Recently, it was discovered^{12,13} that the T' phase $L_2\text{CuO}_4$ ($L = \text{Nd, Sm, Pr}$), whose structure is identical to that of Gd_2CuO_4 , can be doped instead with electrons in the Cu-O₂ planes by substitution of Ce into the L site. T_c as high as 24 K has been achieved in these systems. The above results indicate that doping of holes or electrons onto a Cu-O₂ plane strongly depends on the local geometry of the Cu-O polyhedron. In this respect, the $L_2\text{CuO}_4$ system is an ideal one to study the electronic and superconducting properties of a two-dimensional system, because of the existence of several local Cu-O units.

IV. SUMMARY AND CONCLUSIONS

In summary, the value of T_c in the T -phase solid solution $(\text{La}_{1-x}\text{Gd}_x)_{1.85}\text{Sr}_{0.15}\text{CuO}_4$ ($0 \leq x \leq 0.1$) decreases linearly with Gd substitution, with an extrapolated critical concentration of $x_c = 0.2$. The suppression of T_c strongly correlates with the low-temperature resistivity anomaly which is manifested in a resistivity minimum and upturn. Analysis of the resistivity anomaly shows that it can be best described by a logarithmic temperature dependence. Even though Gd substitution does not occur in the Cu-O₂ plane, structural disorder in the conducting Cu-O₂ plane is induced as revealed in the residual resistivity. Elastic scattering in the form of residual resistivity is not the dominant pair-breaking mechanism. The electron-boson coupling strength remains primarily constant, therefore the suppression of T_c is not due to any reduction in the coupling strength. A room-temperature structural phase diagram indicates that three stable phases exist in $(\text{La}_{1-x}\text{Gd}_x)_{1.85}\text{Sr}_{0.15}\text{CuO}_4$ ($0 \leq x \leq 1$) (the T , T^* , and T' phase) with different local Cu-O structural

units. The Jahn-Teller distortion is significantly reduced in the order of T , T^* , and T' . The T and T^* phases are paramagnetic with a full Gd^{3+} magnetic moment. The T' phase Gd_2CuO_4 or $\text{Gd}_{1.85}\text{Sr}_{0.15}\text{CuO}_4$ has one Néel state associated with the Cu-O₂ plane and another magnetic ordering due to the Gd sublattice. Both resistivity and susceptibility measurements indicate that extra hole carriers cannot be doped onto the Cu-O₂ plane in the T' phase. Recently, Takagi *et al.*,¹² however, have shown that the Cu-O₂ plane of the rare-earth T' phase can be doped with electrons. These results suggest that the ability of doping strongly depends on the local Cu-O units of a perovskite structure.

ACKNOWLEDGMENTS

We would like to thank J. Ruvald, Z. Tesanovic, R. L. Greene, and A. J. Millis for useful discussions. This work was supported by the National Science Foundation through Grant No. DMR 88-22559.

*Current address: Department of Physics, Brown University, Providence, RI 02912.

¹A. W. Sleight, *Science* **242**, 1519 (1989).

²For reviews, see, e.g., *Solid State Physics*, edited by H. Ehrenreich and D. Turnbull (Academic, New York, 1989); J. C. Phillips, *Physics of High T_c Superconductors* (Academic, New York, 1989).

³J. B. Torrance, Y. Tokura, A. Nazzal, and S. S. P. Parkin, *Phys. Rev. Lett.* **60**, 542 (1988).

⁴T. Siegrist, S. M. Zahurak, D. W. Murphy, and R. S. Roth, *Nature (London)* **334**, 231 (1988).

⁵N. Murayama, E. Sudo, K. Kani, A. Tsuzuki, S. Kawakami, M. Awano, and Y. Torii, *Jpn. J. Appl. Phys.* **27**, L1623 (1988).

⁶J. D. Thompson, S.-W. Cheong, S. E. Brown, Z. Fisk, S. B. Oseroff, M. Tovar, D. C. Vier, and S. Schultz, *Phys. Rev. B* **39**, 6660 (1989); G. M. Luke *et al.*, *Nature (London)* **338**, 49 (1989).

⁷J. B. Torrance, Y. Tokura, A. I. Nazzal, A. Bezinge, T. C. Huang, and S. S. P. Parkin, *Phys. Rev. Lett.* **61**, 1127 (1988).

⁸J. B. Goodenough, *Mater. Res. Bull.* **8**, 423 (1973).

⁹P. Ganguly and C. N. R. Rao, *Mater. Res. Bull.* **8**, 405 (1973).

¹⁰K. K. Singh, P. Ganguly, and C. N. R. Rao, *Mater. Res. Bull.* **17**, 493 (1982).

¹¹H. Muller-Buschbaum and W. Wollschlager, *Z. Anorg. Allg. Chem.* **414**, 76 (1975).

¹²Y. Tokura, H. Tagagi, and S. Uchida, *Nature (London)* **337**, 345 (1989).

¹³H. Takagi, S. Uchida, and Y. Tokura, *Phys. Rev. Lett.* **62**, 1197 (1989).

¹⁴V. J. Emery, *Nature (London)* **337**, 306 (1989).

¹⁵T. M. Rice, *Nature (London)* **337**, 686 (1989).

¹⁶D. W. Murthy *et al.*, *Phys. Rev. Lett.* **58**, 1888 (1987).

¹⁷P. H. Hor *et al.*, *Phys. Rev. Lett.* **58**, 1891 (1987).

¹⁸Gang Xiao, F. H. Streitz, A. Gavrin, and C. L. Chien, *Solid State Commun.* **63**, 817 (1987).

¹⁹Gang Xiao, F. H. Streitz, A. Gavrin, Y. W. Du, and C. L. Chien, *Phys. Rev. B* **35**, 8782 (1987).

²⁰Y. Maeno, T. Tomita, M. Kyogoku, S. Awaji, Y. Aoki, K.

Hoshino, A. Minami, and T. Fujita, *Nature (London)* **328**, 512 (1987).

²¹Gang Xiao, M. Z. Cieplak, A. Gavrin, F. H. Streitz, A. Bakhshai, and C. L. Chien, *Phys. Rev. Lett.* **60**, 1446 (1988).

²²Gang Xiao, M. Z. Cieplak, D. Musser, A. Gavrin, F. H. Streitz, C. L. Chien, J. J. Rhyne, and J. A. Gotaas, *Nature (London)* **332**, 238 (1988).

²³For a review of band-theory calculation, see, e.g., W. E. Pickett, *Rev. Mod. Phys.* **61**, 433 (1989).

²⁴J. M. Tarascon, L. H. Greene, W. R. McKinnon, and G. W. Hull, *Solid State Commun.* **63**, 499 (1987).

²⁵H. Takagi, S. Uchida, H. Eisaki, S. Tanaka, K. Kishio, K. Kitazawa, and K. Fueki, *J. Appl. Phys.* **63**, 4009 (1988).

²⁶G. W. Crabtree, W. K. Kwok, A. Umezawa, L. Soderholm, L. Morss, and E. E. Alp, *Phys. Rev. B* **36**, 5258 (1987).

²⁷R. M. Fleming, B. Batlogg, R. J. Cava, and E. A. Rietman, *Phys. Rev. B* **35**, 7191 (1987).

²⁸H. Sawa *et al.*, *Nature (London)* **337**, 347 (1989).

²⁹D. Vaknin, S. K. Sinha, D. E. Moncton, D. C. Johnston, J. M. Newsam, C. R. Safinya, and H. E. King, Jr., *Phys. Rev. Lett.* **58**, 2802 (1987).

³⁰S. Mitsuda, G. Shirane, S. K. Sinha, D. C. Johnston, M. S. Alvarez, D. Vaknin, and D. E. Moncton, *Phys. Rev. B* **36**, 822 (1987).

³¹T. Fujita, Y. Aoki, Y. Maeno, J. Sakurai, H. Fukuba, and H. Fujii, *Jpn. J. Appl. Phys.* **26**, L202 (1987).

³²R. J. Birgeneau, M. A. Kastner, and A. Aharony, *Z. Phys. B* **71**, 57 (1988).

³³D. C. Johnston, *Phys. Rev. Lett.* **62**, 957 (1989).

³⁴J. M. Tarascon, W. R. McKinnon, L. H. Greene, G. W. Hull, and E. M. Vogel, *Phys. Rev. B* **36**, 226 (1987).

³⁵M. Gurvitch and A. T. Fiory, *Phys. Rev. Lett.* **59**, 1337 (1987).

³⁶P. A. Lee and N. Reed, *Phys. Rev. Lett.* **58**, 2691 (1987).

³⁷Gang Xiao, A. Bakhshai, M. Z. Cieplak, Z. Tesanovic, and C. L. Chien, *Phys. Rev. B* **39**, 315 (1989).

³⁸L. Coffey and D. L. Cox, *Phys. Rev. B* **37**, 3389 (1988).

³⁹J. Kondo, *Solid State Physics*, edited by H. Ehrenreich, F. Seitz, and D. Turnbull (Academic, New York, 1969), Vol. 23, p. 183; A. J. Heeger, *ibid.*, p. 283.

- ⁴⁰C. Kittel, *Introduction to Solid State Physics*, (Wiley, New York, 1986), p. 598.
- ⁴¹P. A. Lee and T. V. Ramakrishnan, *Rev. Mod. Phys.* **57**, 287 (1985).
- ⁴²M. Z. Cieplak, Gang Xiao, A. Bakhshai, and C. L. Chien, *Phys. Rev. B* **39**, 4222 (1989).
- ⁴³Gang Xiao, M. Z. Cieplak, A. Bakhshai, C. L. Chien (unpublished).
- ⁴⁴A. Hofmann, H. Kronmüller, N. Moser, R. Reisser, P. Schüle, and F. Dworschak, *Physica C* **156**, 528 (1988).
- ⁴⁵A. A. Abrikosov and L. P. Gor'kov, *Zh. Eksp. Teor. Fiz.* **39**, 1781 (1960) [*Sov. Phys.—JETP* **12**, 1243 (1961)].